LBNL–42276
OM-394

Presented at the Third International Meeting on Electrochromics in London, England, September 8, 1998 and accepted for publication in Electrochimica Acta.

Electrochromic Lithium Nickel Oxide Thin Films by RF-Sputtering from a $LiNiO_2$ Target

F. Michalak, K. von Rottkay, T. Richardson, J. Slack, M. Rubin

Windows and Daylighting Group
Building Technologies Department
Environmental Energy Technologies Division
Ernest Orlando Lawrence Berkeley National Laboratory
University of California
Berkeley, CA 94720

September 1998

This work was supported by the Assistant Secretary for Energy Efficiency and Renewable Energy, Office of Building Technology, State and Community Programs, Office of Building Systems of the U.S. Department of Energy under Contract No. DE-AC03-76SF00098.

Electrochromic Lithium Nickel Oxide Thin Films by rf-sputtering from a $LiNiO_2$ Target

F. Michalak, K. von Rottkay, T. Richardson, J. Slack, M. Rubin
Lawrence Berkeley National Laboratory, Berkeley CA 94720, USA.

Abstract
Thin films of lithium nickel oxide were deposited by rf-sputtering from a stoichiometric $LiNiO_2$ target. The composition and structure of these films depended on the oxygen pressure during deposition (sputtering gas is Argon), and, to a certain extent, the target history. The sputtering geometry, i.e. the substrate to target distance and the sputtering angle were also critical. The films exhibit excellent reversibility in the potential range 1.1V to 3.8V vs Li/Li^+, and could be cycled in a liquid electrolyte half cell for more than 3000 cycles with a switching range ΔT_{vis} close to 70%. The coloration efficiency in the visible was typically –30 to -40 $cm^2 C^{-1}$. The switching performance of a device utilizing a lithium nickel oxide film as counter electrode for a tungsten oxide electrochromic film is reported.

1. Introduction
Non-stoichiometric nickel oxide (LiNiO) is an intercalation electrode with remarkable electrochemical and optical properties.[1-11] It has a wide span of transmittance between the clear and dark states which makes possible its use in a variety of electrochromic applications, including use as a privacy screen; it is color-neutral in both states; it exhibits fast switching, high coloration efficiency (CE), and excellent cycling stability. A wide variety of deposition conditions for LiNiO thin films have been reported in the literature[21], including DC reactive sputtering with or without the presence of H_2, rf-sputtering from N_iO_x and pulsed laser deposition from $LiNiO_2$. Testin conditions have also been highly variable, making comparisons difficult. All of the materials reported to date require some kind of formatting step that differs from the "normal" cycling conditions. Bulk lithium nickel oxides consist of close-packed oxide ions with cations in the octahedral sites. $Li_xNi_{1-x}O$ ($x<0.3$), is a substitutional solid solution with a cubic NiO-like structure.[22, 23, 24] For $x>0.3$, the structure is hexagonal due to ordering of the cations in alternating layers within the oxide lattice.[15, 20, 25-28] It is commonly denoted as $Li_{2x}Ni_{2-2x}O_2$ to point out the structural difference. In both forms, cation vacancies may exist. Lithium ions ma be inserted or extracted with accompanying reduction or oxidation of nickel. Electrochromic switching in LiNiO materials involves the Ni^{3+}(dark)/Ni^{2+} (transparent) redox couple. Thus, the nickel ions must be at or near an average oxidation state of '2' when the films are bleached. Assuming the absence of oxide ion vacancies, this requires insertion of more lithium ions than there are vacancies in the nickel sites. The additional lithium ions presumably occupy tetrahedral sites, which may give them lower mobility. This may take place during the formatting process, which involves some irreversible insertion of lithium. In an effort to develop a film that would require little or no formatting, we used a starting material, $LiNiO_2$, that already contains lithium. In a previous work[29], PLD was used to produce thin films from this material. In this paper we report the electrochromic properties of thin films produced by rf magnetron sputtering of stoichiometric $LiNiO_2$.

2. Experimental

2.1 Thin film deposition

$LiNiO_2$ films were produced by RF magnetron reactive sputtering from a 1.5" diameter $LiNiO_2$ target (Superconductive Components, Inc.), which was shown by X-ray diffraction (XRD) to be single-phase and stochiometric. The deposition chamber was maintained at ultimate base pressures ranging from 6×10^{-8} to 3×10^{-7} Torr, pumped by a CTI CRYO-TORR 8 cryo-pump. SnO_2:F-coated glass substrates were ultrasonically cleaned for 10 m in a 1:16 solution of Liquinox® detergent, thoroughly rinsed in de-ionized water, and dried under flowing N_2. The substrates were further dried by heating in the load lock to 110°C at 5×10^{-5} Torr, transferred into the main chamber and plasma etched using an AtomTech source for two minutes at 50 W. The target was pre-sputtered for 20 minutes at the anticipated run pressure and 20% O_2 concentration. Gas flow rates were 96 sccm Ar and 24 sccm O_2. Deposition pressures ranged from 30 to 60 mTorr. Sputtering was off-angle, with the sputter gun inclined 15° from normal. Target to substrate centerline distance was 10.4 cm. Deposition times ranged between 90 and 120 min at 80 W RF power. Deposition rates were approximately 13 Å min^{-1} at 30 mTorr and 8 Å min^{-1} at 60 mTorr. Deposited samples were removed from the load lock into a vacuum purged and Argon backfilled glovebag, heat sealed into double plastic bags while still in Ar, and transferred into the glovebox within an hour of removal. Table 1 summarizes the sputtering conditions for the samples used in this work. Ni412a was used to make a WO_3/LiNiO device.

Table 1: Sputtering conditions

Sample	Pressure	O_2 Conc.	Run time	Thickness (Å)	Rate (Å min^{-1})
Ni412a	30 mTorr	20%	105 min	1350	12.9
Ni417a	30 mTorr	20%	90 min	1100	12.2
Ni420	60 mTorr	20%	120 min	1000	8.3

2.2 XRD Characterization

Grazing angle XRD patterns were obtained using a Siemens D500 diffractometer using Cu K_α radiation with a position sensitive detector and an incident angle of 0.5°.

2.3 Optical testing

Spectrophotometric measurements from 250 nm to 2500 nm were taken at near-normal incidence on a Perkin-Elmer Lambda 19 spectrophotometer.

2.4 Electrochemical film testing

Films were transferred to a He filled glove box (water, O_2 <1ppm) for electrochemical testing. The three electrode cell was filled with 1M $LiClO_4$ in propylene carbonate (EM Merck, battery grade). A tungsten halogen light source brought into the glove box via optical fiber and a Si detector equipped with a photoptic filter (International Light) allowed us to measure the visible transmittance *in situ*. Two pieces of lithium foil were used as counter and reference electrodes. The electrochemical cell and the output of the detector were connected to an Arbin battery testing system.

2.5 Devices

Two devices comprising thin film electrodes and a transparent gel electrolyte were prepared to compare the performance of tungsten oxide using optically passive and active counter-electrodes. Each electrode was characterized independently before the devices were assembled. The first device used a sol-gel vanadium oxide counter electrode with a coloration efficiency of ca. 3 cm^2 C^{-1}. The second incorporated a sputtered lithium nickel oxide electrode (C.E. = 28 cm^2 C^{-1}). The capacities of the counter electrodes were approximately matched to those of the tungsten oxide electrodes (Donnelly Corp., C. E. = 43 cm^2 C^{-1}). The devices employed a 125μm thick porous polyvinylidenedifluoride (PVDF) separator (Gelman FPVericel 200) containing ca. 90 ^{w}/o $LiClO_4$/propylene carbonate electrolyte. The devices were assembled in the dry box, and the edges were sealed using low vapor pressure epoxy (Torr Seal, Varian Associates). The active area of each cell was 7.0 cm^2. The devices were cycled at a rate of 2 mV s^{-1} between experimentally determined limits.

3. Results

3.1 XRD Characterization

The diffraction pattern from a 2 μm thick LiNiO film is shown in Figure 1. The most intense peaks are due to the pseudo-cubic $Li_xNi_{1-y}O$ phase. No evidence is seen for a layered nickel oxide. In addition, a significant quantity of lithium carbonate is present. This presumably arises from reaction of atmospheric CO_2 with lithium oxide present as a second phase in the sputtered film. Li_2CO_3 is absent from the pattern obtained following electrochemical cycling of the film in the glovebox.

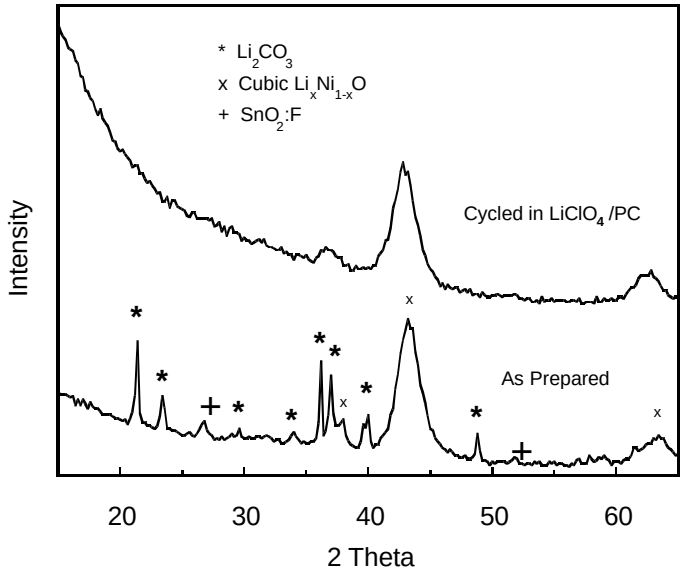

Figure 1: X-ray diffraction patterns from LiNiO film on SnO_2:F-coated glass.

3.2 Optical measurements

Figure 2 shows the spectral transmission in the dark state of Li_xWO_3 and LiNiO. These two materials are complementary in the visible and the near IR, and pairing them in a complete device results in a very dark, color neutral system. This deserves attention, since the typical

bluish tint of Li_xWO_3 is often perceived as objectionable. The spectral optical constants of both LiNiO and Li_xWO_3 films as a function of intercalated Li^+ were reported previously.[30,31]

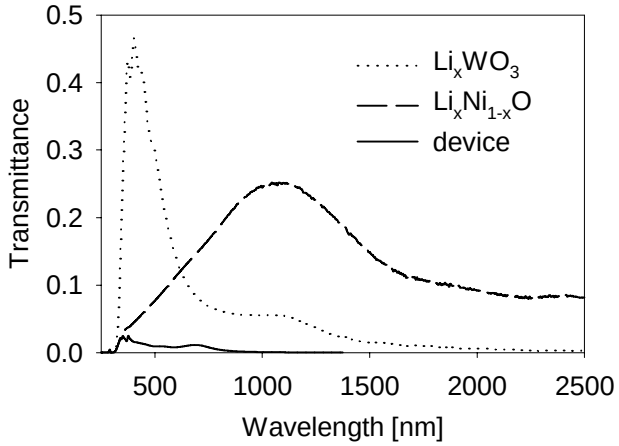

Figure 2: Dark state spectra of Li_xWO_3 and LiNiO on ITO-coated glass.

3.3 Half cells

Figure 3 shows the first 5 cycles of a lithium nickel oxide (sample number Ni417). The sample was cycled between 3.8 and 1.1 V vs Li/Li^+ at 10mV s^{-1}. The first cycle shows an extra cathodic charge along with a slower bleaching. This "formatting" is limited to the first half cycle and does not require any special cycling conditions. Subsequent cycles are nearly identical to one another. The visible transmission changes from ca 15% in the dark state to 83% in the clear state with a CE of about 40 cm^2 C^{-1}. Figure 4 shows the 20^{th} and 152^{nd} cycles of the same sample. Figure 5 shows the transmission data for 150 cycles. Both the dark and the clear states remain remarkably stable at 16% and 82% respectively.

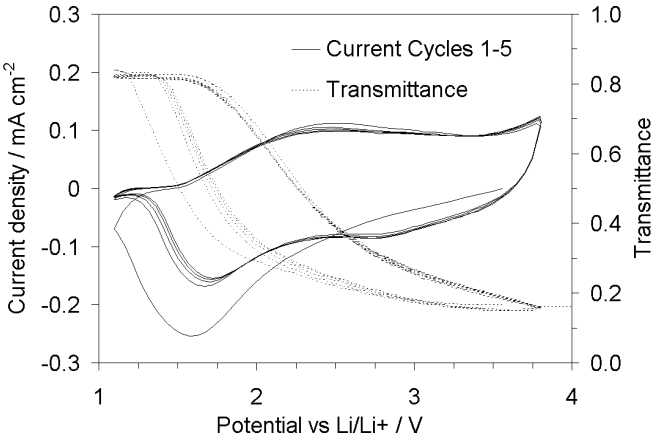

Figure 3: Cycles 1-5 of LiNiO electrode in 1M LiClO4 in PC at 10 mV s^{-1}.

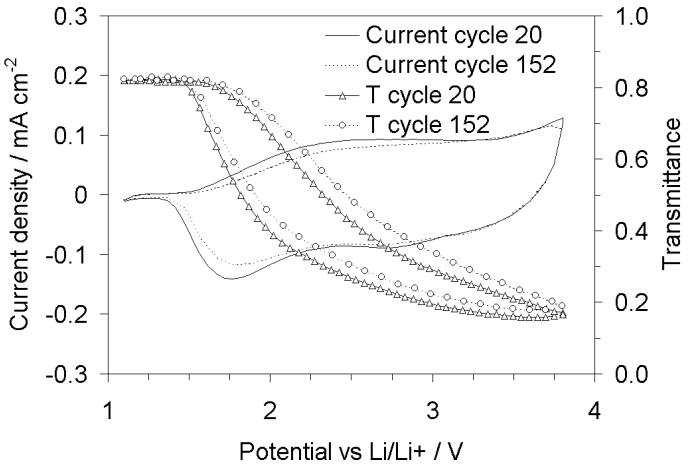

Figure 4: 20th cycle of a LiNiO electrode in 1M LiClO4 in PC at 10 mV s^{-1}.

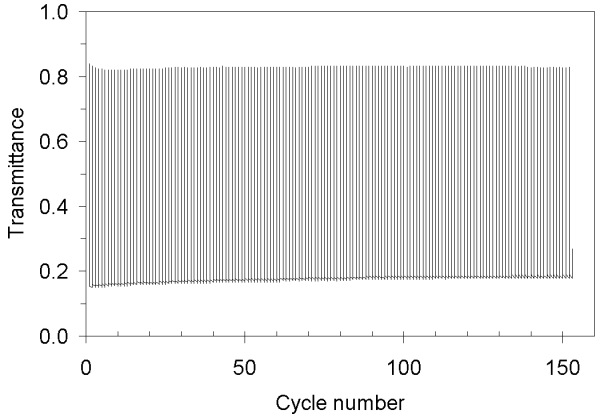

Figure 5: % T versus time for 150 cycles.

3.4 Devices

WO_3/V_2O_5 and WO_3/LiNiO cells were assembled to demonstrate the advantage of using LiNiO as a counter electrode over V_2O_5. The WO_3/V_2O_5 cell switched between 65 and 17% T (Figure 6), with a coloration efficiency of 42 cm^2 C^{-1}, essentially that of the tungsten oxide film. The WO_3/LiNiO device switched between 65 and 8% T with excellent cycle-to-cycle stability (Figure 7) and a high coloration efficiency (56 cm^2 C^{-1}). By extending the voltage limits, a larger switching range could be achieved (Figure 8), although the repeatability of the switching was slightly degraded. After the cell was polarized sufficiently to darken it to 1-2% T, the shapes of the cycling curves were altered (Figure 9). Large anodic and cathodic peaks appeared near the potential extremes and the optical switching hysteresis increased. While the darkening continued to occur in a smooth fashion, the bleaching process became much more delayed and developed two distinct steps, possibly due to markedly different bleaching rates for the two electrodes. The overall coloration efficiency increased to 65 cm^2 C^{-1}.

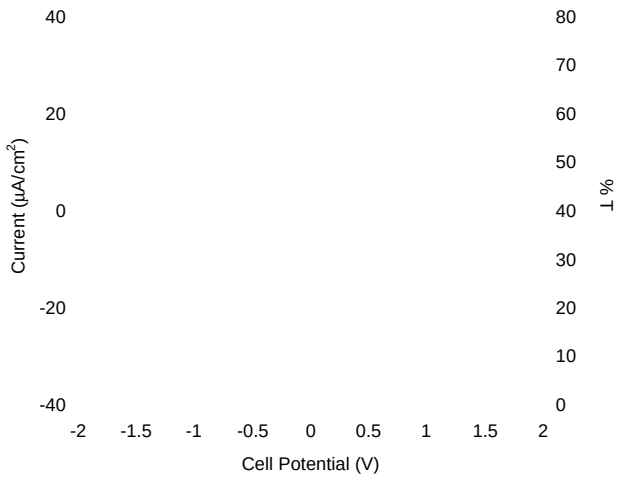

Figure 6: Electrochromic switching behavior of WO_3/V_2O_5 device. Scan rate 2 mV s^{-1}.

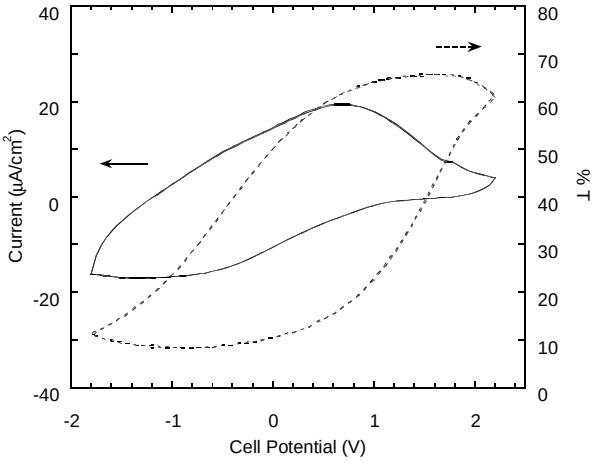

Figure 7: Electrochromic switching behavior of WO_3/LiNiO device. Scan rate 2 mV s^{-1}.

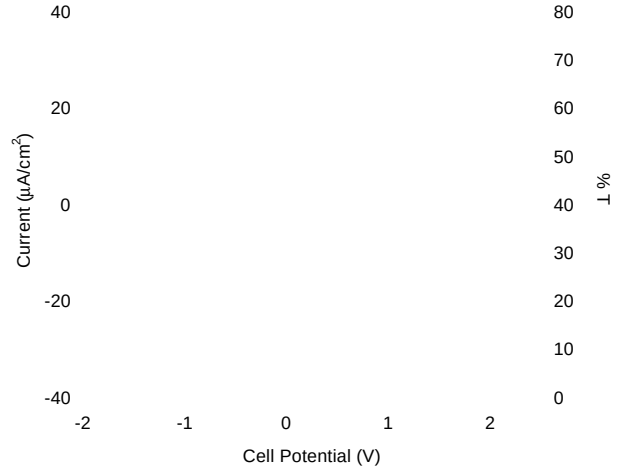

Figure 8: Electrochromic switching behavior of WO_3/LiNiO device. Scan rate 2 mV s^{-1}.

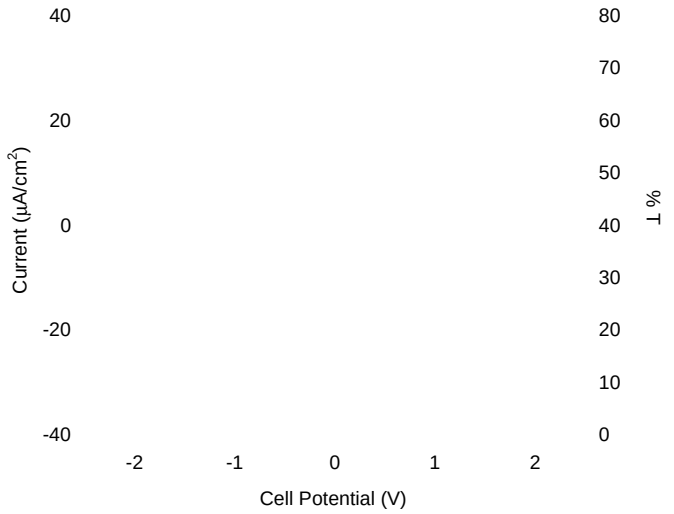

Figure 9: Electrochromic switching behavior of WO_3/LiNiO device. Scan rate 2 mV s^{-1}.

4. Conclusion

LiNiO thin films produced by rf-sputtering from a stochiometric $LiNiO_2$ target exhibit good electrochromic properties as well as excellent stability. The ability to produce a "privacy level" dark state by combining the LiNiO films with a typical tungsten oxide film was demonstrated in a gel electrolyte device. Stable and repeatable switching between 75 % and 2% T with color neutrality was achieved. While there are still issues of reproducibility in the sputtering process, and the need for formatting has not yet been eliminated, lithium nickel oxide films have been shown to be very useful optically active counter electrodes for window applications.

5. Acknowledgment

This work was supported by the Assistant Secretary for Energy Efficiency and Renewable Energy, Office of Building Technology, State and Community Programs, Office of Building Systems of the U.S. Department of Energy under Contract No. DE-AC03-76SF00098.

6. References

1. Pennisi, C.M. Lampert, *Proc. SPIE,* **1016,** 131 (1988).
2. S.I. Cordoba-Torresi, A. Hugot-LeGoff, S. Joiret, *J. Electrochem. Soc*., **138,** 1554 (1991).
3. J. Nagai, *Proc. SPIE,* **1728,** 194 (1992).
4. C. Arbizziani, M. Mastragostino, S. Passerini, R. Pileggi, B. Scrosati, *Electrochim. Acta,* **36**, 837 (1991).
5. G. Campet, B. Morel, M. Bourrel, J.M. Chabagno, D. Ferry, R. Garie, C. Quet, C. Geoffroy, J. Portier, C. Delmas, J. Salardenne, *Mater. Sci. Engr. B*, **8**, 303 (1991)
6. J. Scarminio, A. Gorenstein, F. Decker, S. Passerini, R. Pileggi, B. Scrosati, *Proc. SPIE,* **1536**, 70 (1991).
7. F. Decker, S. Passerini, R. Pileggi, B. Scrosati, *Electrochim. Acta,* **37**, 1033 (1992).
8. S. Passerini, B. Scrosati, *Solid State Ionics,* **53-56**, 520 (1992).
9. S. Passerini, B. Scrosati, A. Gorenstein, *J. Electrochem. Soc.*, **137**, 3297 (1990).
10. S. Passerini, B. Scrosati, *J. Electrochem. Soc*., **141**, 889 (1994).

11. S. Passerini, B. Scrosati, A. Gorenstein, A.M. Andersson, C.-G. Granqvist, *J. Electrochem. Soc.*, **136**, 3394 (1989).
12. C.B. Azzoni, A. Paleari, V. Massarotti, M. Bini, D. Capsoni, *Phys. Rev. B,* **53,** 703 (1996).
13. W. Li, J.N. Reimers, J.R. Dahn, , *Phys. Rev. B,* **46**, 3236 (1992).
14. I.J. Pickering, J.T. Lewandowski, A.J. Jacobson, J.A. Goldstone, *Solid State Ionics*, **53-56**, 405 (1992).
15. D. Rahmer, S. Machill, H. Schlörb, K. Siury, M. Kloss, W Plieth, *J. Solid State Electrochem.*, **2**, 78 (1998).
16. A. Rougier, C. Delmas, A.V. Chadwick, *Solid State Commun.*, **94**, 123 (1995).
17. J.N. Reimers, W. Li, J.R. Dahn, , *Phys. Rev. B,* **47**, 8486 (1993).
18. J.R. Dahn, U. von Sacken, C.A. Michal, *Solid State Ionics,* **44**, 87 (1990).
19. R. Stoyanova, E. Zhecheva, S. Angelov, *Solid State Ionics*, **59**, 17 (1993).
20. A. Rougier, A.V. Chadwick, C. Delmas, *Nucl. Instr. Meth. Phys. Res. B,* **97**, 75 (1995).
21. C.G. Granqvist, *Handbook of Inorganic Electrochromic Materials,* Elsevier (1995).
22. C.B. Azzoni, A. Paleari, V. Massarotti, M. Bini, D. Capsoni, *Phys. Rev. B,* **53**, 703 (1996).
23. W. Li, J.N. Reimers, J.R. Dahn, *Phys. Rev. B,* **46**, 3236 (1992).
24. I.J. Pickering, J.T. Lewandowski, A.J. Jacobson, J.A. Goldstone, *Solid State Ionics*, **53-56**, 405 (1992).
25. A. Rougier, C. Delmas, A.V. Chadwick, *Solid State Comm.*, **94**, 123 (1995).
26. J.N. Reimers, W. Li, J.R. Dahn, *Phys. Rev. B,* **47**, 8486 (1993).
27. J.R. Dahn, U. von Sacken, C.A. Michal, *Solid State Ionics,* **44**, 87 (1990).
28. R. Stoyanova, E. Zhecheva, S. Angelov, *Solid State Ionics,* **59** (1993). 17
29. M. Rubin, S.-J. Wen, T. Richardson, J. Kerr, K. von Rottkay, J. Slack, *Sol. Ener. Mater. Sol. Cells*, **54**, 59 (1998).
30. M. Rubin, K. von Rottkay, S.-J. Wen, N. Ozer, J. Slack, *Sol. Ener. Mater. Sol. Cells*, **54**, 49 (1998).
31. K. von Rottkay, M. Rubin, S.-J. Wen, *Thin Solid Films*, **306**, 10 (1997).